Observational tests of a two parameter power-law class modified gravity in Palatini formalism

Shant Baghram,[1] M. Sadegh Movahed,[2,3] and Sohrab Rahvar[1]

[1]*Department of Physics, Sharif University of Technology, P.O. Box 11365–9161, Tehran, Iran*

[2]*Department of Physics, Shahid Beheshti university, G.C., Evin, Tehran 19839, Iran*

[3]*School of Astronomy and Astrophysics, Institute for Research in Fundamental Sciences, (IPM), P. O. Box 19395-5531, Tehran, Iran*

(Received 24 April 2009; published 1 September 2009)

CONTEXT: In this work we propose a modified gravity action $f(R) = (R^n - R_0^n)^{1/n}$ with two free parameters of n and R_0 and derive the dynamics of a universe for this action in the Palatini formalism. *AIM*: We do a cosmological comparison of this model with observed data to find the best parameters of a model in a flat universe. *METHOD*: To constrain the free parameters of model we use SNIa type Ia data in two sets of gold and union samples, CMB-shift parameter, baryon acoustic oscillation, gas mass fraction in cluster of galaxies, and large-scale structure data. *RESULT*: The best fit from the observational data results in the parameters of model in the range of $n = 0.98^{+0.08}_{-0.08}$ and $\Omega_M = 0.25^{-0.1}_{+0.1}$ with one sigma level of confidence where a standard ΛCDM universe resides in this range of solution.

DOI: 10.1103/PhysRevD.80.064003 PACS numbers: 04.50.−h, 95.36.+x, 98.80.−k

I. INTRODUCTION

Recent observation of CMB + SNIa reveals that the Universe is under positive acceleration, in contrast to our expectations from the behavior of ordinary matter. One of the possible solutions is assuming a cosmological constant to provide a late time acceleration to the universe [1]. Although ΛCDM is the easiest model that fits well with the current observational data, it suffers from the fine-tuning and coincidence problems, which motivates to introduce alternative theories such as dark energy models. The other possibility is the modification of gravity law in such a way that behaves as standard general relativity in a strong gravitational regime, but repulses particles in the cosmological scales [2]. Each proposed model must challenge two different observational criteria of (a) cosmological tests and (b) local gravity tests in solar system scales.

In this work we examine a $f(R) = (R^n - R_0^n)^{1/n}$ gravity model with the cosmological observational data to fix the two parameters of the model, R_0 and n. We use Supernova Type Ia, CMB shift parameter, baryonic acoustic oscillation, gas mass fraction in cluster of galaxies, and large scale structures to find the best parameter of the model. The organization of paper is as follows: In Sec. II we introduce the field equation in a $f(R)$ modified gravity model in Palatini formalism. Using the Friedman-Robertson-Walker (FRW) metric we derive a modified Friedman equation. In Sec. III we apply our proposed action to derive the field equations. In Sec. IV we study geometrical and dynamical behavior of a universe in this model. In Sec. V, using the geometrical observations as SNIa, CMB-shift parameter, baryon acoustic oscillation, gas mass fraction of clusters of galaxies, we put constraints on the parameters of the model. Finally, we do a comparison of the model with the large scale structures' data in Sec. V. The conclusions are given in Sec. VI. We show that the best parameter of this model is the privilege of a ΛCDM universe.

II. MODIFIED GRAVITY IN PALATINI FORMALISM

For an arbitrary action of the gravity as a function of Ricci scalar $f(R)$, there are two main approaches to extract the field equations. The first one is the so-called metric formalism, which is obtained by the variation of action with respect to the metric. In this formalism, in contrast to the Einstein-Hilbert action, the field equation is a fourth order nonlinear differential equation. In the second approach, the so-called Palatini formalism, the connection and metric are considered independent fields and variation of action with respect to these fields results in a set of second order differential equations. In what follows we will work in the Palatini formalism. Let us take the general form of action in the Palatini formalism as

$$S[f; g, \hat{\Gamma}, \Psi_m] = \frac{1}{2\kappa}\int d^4x\sqrt{-g}f(R) + S_m[g_{\mu\nu}, \Psi_m], \tag{1}$$

where $\kappa = 8\pi G$ and $S_m[g_{\mu\nu}, \Psi_m]$ is the matter action that depends on metric $g_{\mu\nu}$ and the matter fields Ψ_m. $R = R(g, \hat{\Gamma}) = g^{\mu\nu}R_{\mu\nu}(\hat{\Gamma})$ is the generalized Ricci scalar and $R_{\mu\nu}$ is the Ricci tensor, made of affine connection. Varying action with respect to the metric results in

$$f'(R)R_{\mu\nu}(\hat{\Gamma}) - \tfrac{1}{2}f(R)g_{\mu\nu} = \kappa T_{\mu\nu}, \tag{2}$$

where prime is the differential with respect to the Ricci scalar and $T_{\mu\nu}$ is the energy-momentum tensor

$$T_{\mu\nu} = \frac{-2}{\sqrt{-g}}\frac{\delta S_m}{\delta g^{\mu\nu}}. \tag{3}$$

On the other hand, varying the action with respect to the

connection results in

$$\hat{\nabla}_{\alpha}[f'(R)\sqrt{-g}g^{\mu\nu}] = 0, \tag{4}$$

where $\hat{\nabla}$ is the covariant derivative defined from parallel transformation and depends on affine connection. From Eq. (4), we can define a new metric of $h_{\mu\nu} = f'(R)g_{\mu\nu}$ conformally related to the physical metric where the connection is the Christoffel symbol of this new metric. We take a flat FRW metric (namely $K = 0$) for the universe

$$ds^2 = -dt^2 + a(t)^2\delta_{ij}dx^i dx^j, \tag{5}$$

and assume that universe is filled with a perfect fluid with the energy-momentum tensor of $T^{\nu}_{\mu} = \mathrm{diag}(-\rho, p, p, p)$. Using the metric and energy-momentum tensor in Eq. (2) we obtain the generalized FRW equations. It should be noted that the conservation law of energy-momentum tensor, $T^{\mu\nu}{}_{;\mu} = 0$ is defined according to the covariant derivative with respect to the metric to guarantee the motion of particles on geodesics [3]. A combination of G^0_0 and G^i_i results in

$$\left(H + \frac{1}{2}\frac{\dot{f}'}{f'}\right)^2 = \frac{1}{6}\frac{\kappa(\rho + 3p)}{f'} + \frac{1}{6}\frac{f}{f'}. \tag{6}$$

On the other hand, the trace of Eq. (2) gives

$$Rf'(R) - 2f(R) = \kappa T, \tag{7}$$

where $T = g^{\mu\nu}T_{\mu\nu} = -\rho + 3p$. The time derivative of this equation results in $\dot{R}$ in terms of the time derivative of density and pressure. Using the equation of state of cosmic fluid $p = p(\rho)$ and continuity equation, the time derivative of Ricci is obtained as

$$\dot{R} = 3\kappa H\frac{(1 - 3dp/d\rho)(\rho + p)}{Rf'' - f'(R)}. \tag{8}$$

To obtain a generalized first FRW equation, we start with Eq. (7) and obtain the density of matter in terms of the Ricci scalar as

$$\kappa\rho = \frac{2f - Rf'}{1 - 3\omega}, \tag{9}$$

where $w = p/\rho$. Substituting Eq. (9) in (6) and using Eq. (8) to change $d/dt = \dot{R}d/dR$, we obtain the dynamics of the universe in terms of the Ricci scalar as

$$H^2 = \frac{1}{6(1 - 3\omega)f'}\frac{3(1 + \omega)f - (1 + 3\omega)Rf'}{[1 + \frac{3}{2}(1 + \omega)\frac{f''(2f - Rf')}{f'(Rf'' - f')}]^2}. \tag{10}$$

On the other hand, using Eq. (7) and the continuity equation, the scale factor can be obtained in terms of the Ricci scalar

$$a = \left[\frac{1}{\kappa\rho_0(1 - 3\omega)}(2f - Rf')\right]^{-(1/3(1+\omega))}, \tag{11}$$

where ρ_0 is the energy density at the present time and a_0, the scale factor at the present time, is set to 1. Now for a generic modified action, eliminating the Ricci scalar in favor of the scale factor between Eqs. (10) and (11) we can obtain the dynamics of the universe [i.e. $H = H(a)$]. For the simple case of matter dominant epoch $\omega = 0$, these equations reduce to

$$H^2 = \frac{1}{6f'}\frac{3f - Rf'}{[1 + \frac{3}{2}\frac{f''(2f - Rf')}{f'(Rf'' - f')}]^2}, \tag{12}$$

and

$$a = \left[\frac{1}{\kappa\rho_0}(2f - Rf')\right]^{-(1/3)}. \tag{13}$$

III. $F(R) = (R^N - R_0^N)^{1/N}$ GRAVITY

Here in this section we propose a modified gravity action of $f(R) = (R^n - {R_0}^n)^{1/n}$ with the two free parameters where $R_0 > 0$ and $n > 0$. This action is a generalized form of $n = 2$ that has been discussed in [4,5]. This action has a minimum vacuum in an empty universe and a flat Minkowski space is not achievable in this action. This behavior causes an accelerating expansion of the universe for a low density universe. The minimum curvature from the vacuum solution in Eq. (7) is

$$R_v = 2^{1/n}R_0. \tag{14}$$

On the other hand, for the strong gravitational regimes, the action reduces to the Einstein-Hilbert action. To have the asymptotic behavior of action for these two extreme cases we do a Taylor expansion of action around R_v in an almost empty universe and $R_v/R \to 0$ at strong gravitational regimes. For the weak field, the expansion of action results in

$$f(R) = R_v\left(\frac{1}{2}\right)^{1/n} + \left(\frac{1}{2}\right)^{(1/n)-1}(R - R_v) + \left(\frac{1}{2}\right)^{1/n}\frac{n + 1}{R_v}(R - R_v)^2 + \ldots \tag{15}$$

where ignoring higher order terms, we can rewrite this equation as

$$f(R) = R - \Lambda(R_v, n). \tag{16}$$

Here $\Lambda(R_v, n)$ is an effective cosmological constant depends on the curvature in a vacuum and the exponent of action. On the other hand, we expand the action in a strong gravitational regime (e.g. $R \gg R_v$). In this case the action can be written as follows:

$$f(R) = R + \sum_{m=1}^{\infty}\frac{1}{m!}\prod_{k=0}^{m-1}\left(\frac{1}{n} - k\right)(-1)^m\left(\frac{R_0}{R}\right)^{mn}R. \tag{17}$$

Ignoring the higher orders in a strong gravitational field, this action reduce to the Einstein-Hilbert action. So our chosen actions in these two extreme regimes vary from the

Einstein-Hilbert to the Einstein-Hilbert plus cosmological constant.

Let us study the solutions of modified gravity in three common cases of a pointlike source in vacuum space, a universe in radiation, and matter-dominant epochs. For a pointlike source in an empty space, letting $T^{\mu\nu} = 0$ outside the star, we will have a constant Ricci scalar. This means that we will have constant R_v, $f(R_v)$ and $f'(R_v)$ for all the space. With this condition we write the field equation as follows:

$$G_{\mu\nu} = -\frac{1}{2}\left(R_v - \frac{f(R_v)}{f'(R_v)}\right)g_{\mu\nu}, \tag{18}$$

where the coefficient of metric at the right-hand side of the equation plays the role of effective cosmological constant. Substituting the corresponding value for the vacuum from Eq. (14), the effective cosmological constant obtains $\Lambda_{\text{eff}} = 2^{(1/n)-2}R_0$. So the solution of the field equation in the spherically symmetric space results in a Schwarzschild–de Sitter space. The value of R_0 will be fixed in the next section from the cosmological observations.

In the radiation dominated era we have $p = \rho/3$. With this equation of state, the trace of the energy-momentum tensor is zero and it resembles a vacuum solution where the Ricci scalar is constant and equal to $2^{1/n}R_0$. We substitute $f(R)$ and its derivatives in Eq. (6) to have the dynamics of the Hubble parameter as a function of density of the universe

$$H^2 = \frac{2^{(1/n)-2}}{3}(2\kappa\rho + R_0). \tag{19}$$

Analysis for $n = 2$ shows that R_0 is in the order of H_0^2 [4,5]. So for the radiation-dominant epoch, we neglect R_0 in comparison with the density of the universe. Using the continuity equation provides $\rho \propto a^{-4}$, then the scale factor changes with time as $a \propto t^{1/2}$. This result shows no dynamical deviation from the standard cosmology at the early universe.

For the matter-dominant epoch, we calculate the dynamics of the universe for simplicity in terms of a new variable, $X \equiv R/H_0^2$. The action can be written in this new form as

$$f(R) = {H_0}^2 F(X) \tag{20}$$

$$F(X) = (X^n - {X_0}^n)^{1/n} \tag{21}$$

where $X_0 \equiv R_0/H_0^2$ and $H_0 = 100\ \text{h}\,\text{Km/s/Mpc}$. The relation between the derivatives with respect to R and new variable X is related as

$$f'(R) = F'(X), \tag{22}$$

$$f''(R) = \frac{F''(X)}{H_0^2}, \tag{23}$$

where the derivatives in the left-hand side of equations are with respect to the Ricci scalar, but in the right-hand side they are in terms of X, (i.e. $' = \frac{d}{dX}$).

We rewrite Eq. (12) with the new dimensionless parameter X:

$$\mathcal{H}^2(X) = \frac{1}{6F'}\frac{3F - XF'}{(1 + \frac{3}{2}\frac{F''(2F-XF')}{F'(XF''-F')})^2}, \tag{24}$$

where $\mathcal{H}(X) = H/H_0$ is the normalized Hubble parameter to its current value. Using the conventional definition of Ω_m at the present time as $\Omega_m = \kappa\rho_m^{(0)}/3H_0^2$ and Eq. (9) we obtain

$$\Omega_m(X) = \frac{2F - XF'}{3}, \tag{25}$$

where $\Omega_m(X) = \Omega_m a^{-3}$. We obtain the relation between the scale factor and dimensionless parameter X as

$$a = \left(\frac{2F - XF'}{3\Omega_m}\right)^{-1/3}. \tag{26}$$

In order to have positive scale factor, X should change in the range of $X \geq 2^{1/n}X_0$, where the minimum value for X_0 is in agreement with the vacuum solution of the Ricci scalar.

An important point worth mentioning here is that the two free parameters X_0 and n, appeared in the dynamics of the universe can be replaced with more relevant ones. One of them is Ω_m presented in Eq. (25), which relates directly to n, X_0 and X_p (p stands for the present time). X_p can be eliminated using Eq. (24), letting $\mathcal{H}(X_p) = 1$ results in a relation between X_P and X_0 and n. The second parameter we will use instead of X_0 is X_p.

IV. GEOMETRICAL PARAMETERS IN $f(R)$ GRAVITY

The cosmological observations are mainly dependent on background spatial curvature and four dimensional spacetime curvature of the universe. In this section we introduce the geometrical parameters in modified gravity to use in observational tests of the model.

A. Comoving distance

The radial comoving distance is one of the basic parameters in cosmology. For an object with a redshift of z, using the null geodesics in the FRW metric, the comoving distance in terms of X is obtained by

$$r(z; n, X_0) = c\int_0^z \frac{dz'}{H(z')}, \tag{27}$$

$$= \frac{cH_0^{-1}}{3^{4/3}(\Omega_m)^{1/3}}\int_{X_p}^{X}\frac{F' - XF''}{(2F - XF')^{2/3}}\frac{dX}{\mathcal{H}(X)}, \tag{28}$$

where the dimensionless parameter X relates to the redshift

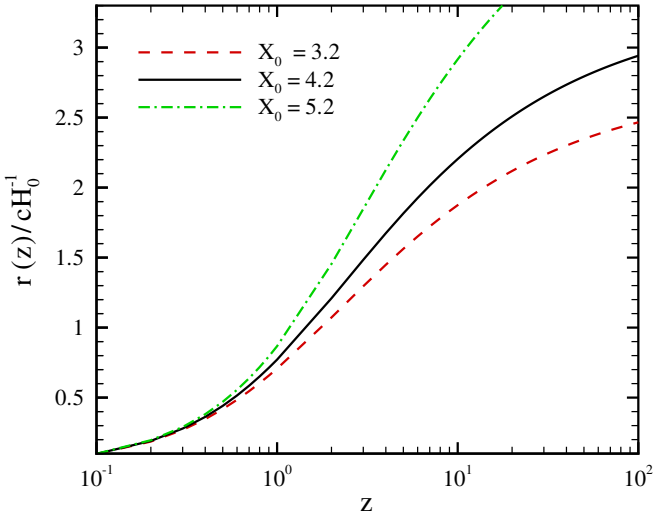

FIG. 1 (color online). The dependence of comoving distance as a function of redshift for the case of $n = 1$ and various X_0. Increasing X_0 makes larger comoving distance for a given redshift.

from Eq. (11) as

$$z = \left[\frac{1}{3\Omega_m}(X^n - X_0^n)^{(1/n)-1}(X^n - 2X_0^n)\right]^{1/3} - 1 \quad (29)$$

Knowing the parameters of the action n and X_0, we can calculate the Hubble parameter at a given X by Eq. (24); substituting it in (28) we obtain a comoving distance by numerical integration. Figures 1 and 2 show comoving distance as a function of redshift in the unit of cH_0^{-1} for various values of parameters of the model. In Fig. 1 we fix $n = 1$ which is equivalent to the ΛCDM universe and let X_0 vary. It seems that X_0 plays the role of effective cosmological constant. Increasing this term makes a larger comoving distance for a given redshift. In Fig. 2 we keep $X_0 = 4.2$ and let n change. Increasing the exponent results in a smaller comoving distance for a given redshift.

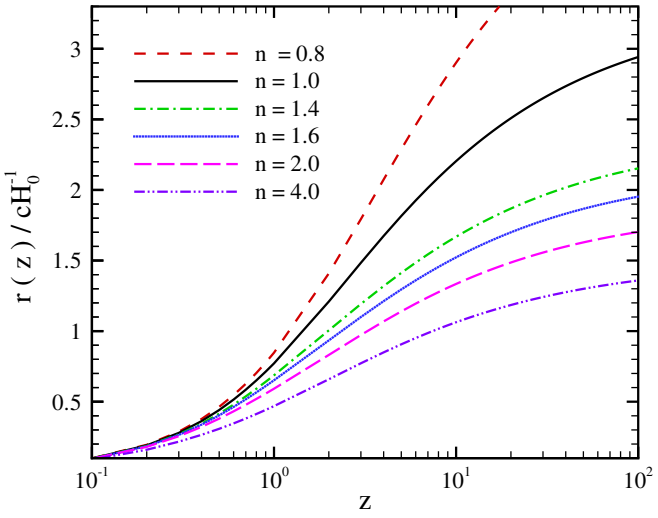

FIG. 2 (color online). The dependence of comoving distance as a function of redshift for the case of $X_0 = 4.2$ and various n. Increasing the exponent results in smaller comoving distance for a given redshift.

B. Angular diameter distance and Alcock-Paczynski test

The apparent angular size of an object located at the cosmological distance is another important parameter that can be affected by the cosmological model. An object at the redshift of z and the perpendicular size of $D_\perp$ is seen by the angular size of

$$\Delta\theta = \frac{D_\perp}{d_A}, \quad (30)$$

where $d_A = r(z; n, X_0)/(1 + z)$ is the angular diameter distance. Now imagine this structure has the size of $D_\parallel$ along our line of sight. Then the light arriving at us from the back and front of this structure will not have the same redshift. The difference in the redshifts of the two sides of the structure can be obtained by the delay in received light to the observer with $\Delta t(z) = D_\parallel/c$. Writing Δt in terms of Δa as $\Delta t = H^{-1}(z)\Delta a/a$ we again change Δa in terms of Δz as $\Delta z/(1 + z) = -\Delta a/a$. The result is writing the width of the structure in redshift space along our line of sight in terms of physical size as

$$\Delta z = \frac{1}{c} D_\parallel H(z)(1 + z). \quad (31)$$

Now the width of the structure in the redshift space to the apparent angular size of structure is obtained as

$$\frac{\Delta z}{\Delta\theta} = \frac{(1 + z)H(z)d_A}{c}\left(\frac{D_\parallel}{D_\perp}\right). \quad (32)$$

For the spherical structures, for instance taking into account the neutral hydrogen clouds at $z < 6$ with the spherical symmetric shape, Eq. (32) is written as

$$\frac{\Delta z}{\Delta\theta} = \frac{H(z; n, X_0)r(z; n, X_0)}{c}. \quad (33)$$

This relation is the so-called Alcock-Paczynski test. The advantage of the Alcock-Paczynski test is that this relation is independent of the Hubble parameter at the present time and of the existence of the dust in the intergalactic medium. In this method, instead of using a standard candle, we will use a standard ruler such as the baryonic acoustic oscillation.

Figures 3 and 4 show a dependence of $\Delta z/\Delta\theta$ as a function of redshift normalized to the corresponding value in a ΛCDM universe. In Fig. 3 the relative size of the structure in redshift space to the observed angular size is compared to that in a ΛCDM universe for a fixed value of $n = 1$. In Fig. 4 we fixed $X_0 = 4.2$ and change the exponent n.

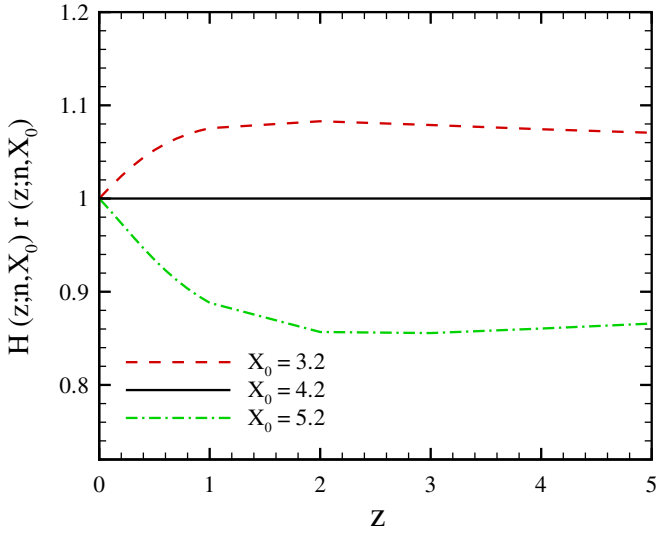

FIG. 3 (color online). The dependence of $\Delta z/\Delta\theta$ as a function of redshift for the case of $n = 1$ and various X_0. Increasing X_0 causes an increase in the apparent size of cosmological objects.

TABLE I. Different priors on the parameter space, used in the likelihood analysis.

Parameter	Prior	
K	0.00	Fixed
$\Omega_b h^2$	0.020 ± 0.005	Top hat (BBN) [36]
h	-	Free [37,38]
w	0	Fixed

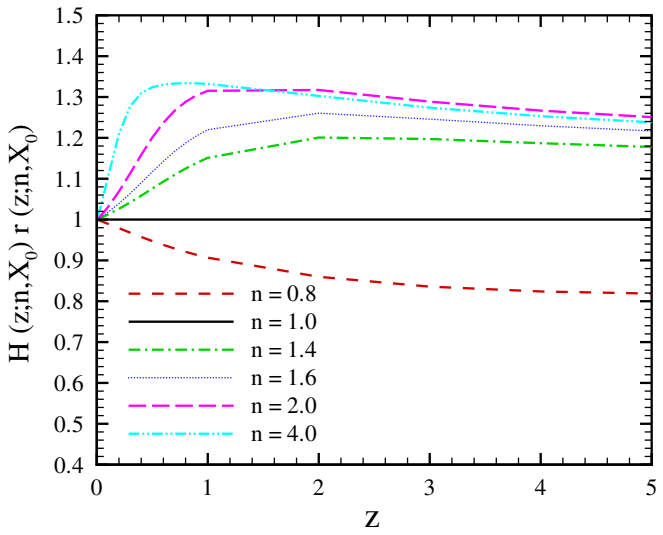

FIG. 4 (color online). The dependence of $\Delta z/\Delta\theta$ as a function of redshift for the case of $X_0 = 4.2$ and various n. Increasing the exponent results in a decrease in the apparent cosmological size of objects.

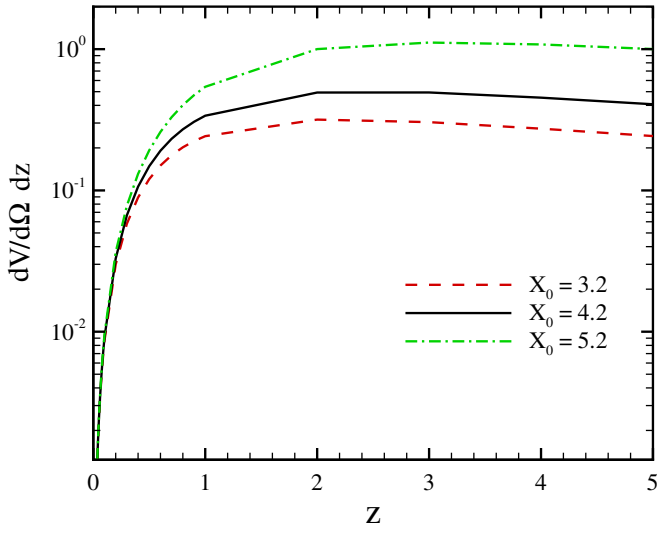

FIG. 5 (color online). The dependence of comoving element as a function of redshift for the case of $n = 1$ and various X_0. Increasing X_0 increases the comoving volume element.

C. Comoving volume element

The comoving volume element is another geometrical parameter that is used in number-count tests such as lensed quasars, galaxies, or clusters of galaxies. The comoving volume element in terms of comoving distance and Hubble parameter is given by

$$f(z; n, X_0) \equiv \frac{dV}{dz d\Omega} = \frac{r^2(z; n, X_0)}{H(z; n, X_0)}. \tag{34}$$

Figures 5 and 6 show the dependence of comoving volume element as a function of redshift. Figure 5 represents the

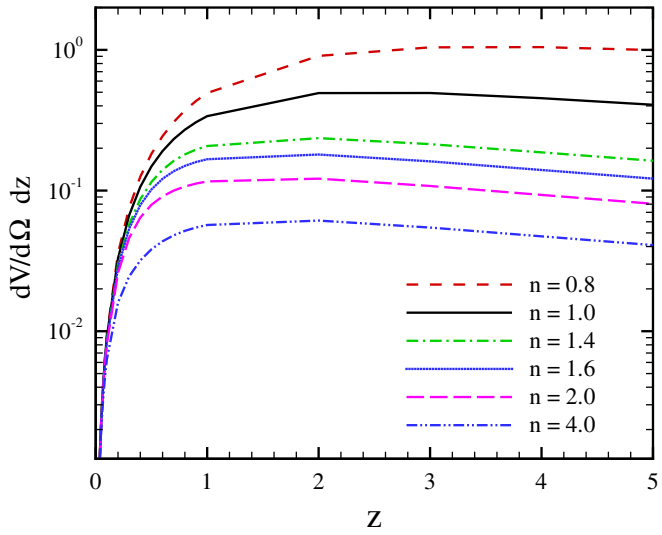

FIG. 6 (color online). The dependence of comoving element as a function of redshift for the case of $X_0 = 4.2$ and various n. Increasing the exponent decreases the comoving volume element.

dependence of comoving volume for a fixed $n = 1$ and various X_0. Increasing X_0 causes a larger comoving volume element. In Fig. 6 we plot the volume for fixed $X_0 = 4.2$ changing n. Increasing the exponent index makes the comoving volume element smaller.

V. OBSERVATIONAL CONSTRAINTS: BACKGROUND EVOLUTION

In this section we compare the observed data with that from the dynamics of the background from the model. We use Supernova Type Ia data, CMB-shift parameter, baryonic acoustic oscillation (BAO), and the gas mass fraction of a cluster of galaxies to constrain the parameters of the model.

A. Supernova type Ia

The Supernova Type Ia experiments provided the main evidence for the existence of dark energy. Since 1995, two teams of High-Z Supernova Search and the Supernova Cosmology Project have discovered several type Ia supernovas at the high redshifts [6,7]. They showed that to interpret the faintness of high redshift supernovas in a flat universe, one has to consider an accelerating universe at the present time.

In this work we take two sets of SNIa data. The first one is the gold sample which has a 157 supernova [8] and the second set is a combined data set of a 192 supernova [9]. The distance modulus for supernovas is calculated by

$$\mu = m - M = 5\log D_L(z; X_0, n) + 5\log\left(\frac{c/H_0}{1\ \mathrm{Mpc}}\right) + 25, \tag{35}$$

where

$$D_L(z; X_0, n) = (1+z)H_0 \int_0^z \frac{dz'}{H(z')}, \tag{36}$$

and D_L can be written in terms of new parameter X, which appeared in the redefinition of the modified gravity action as

$$D_L = \frac{1}{3}\frac{(2F - XF')^{1/3}}{(3\Omega_m)^{2/3}} \int_{X_p}^{X} \frac{F' - XF''}{(2F - XF')^{2/3}} \frac{dX}{\mathcal{H}(X)}. \tag{37}$$

For simplicity in calculation, we define

$$\bar{M} = 5\log\left(\frac{c/H_0}{\mathrm{Mpc}}\right) + 25, \tag{38}$$

which is a function of the Hubble constant at the present time. We write the distance modulus

$$\mu = 5\log D_L(z; X_0, n) + \bar{M}. \tag{39}$$

In the next step we use χ^2 fitting to constrain the parameters of the model.

$$\chi^2(\bar{M}, X_0, n) = \sum_i \frac{[\mu_{\mathrm{obs}}(z_i) - \mu_{\mathrm{th}}(z_i; \bar{M}, X_0, n)]^2}{\sigma_i^2}, \tag{40}$$

where σ_i is the uncertainty in the distance modulus. To constrain the parameters of the model, we use the likelihood statistical analysis:

$$\mathcal{L}(\bar{M}, X_0) = \mathcal{N} e^{-\chi^2(\bar{M}, X_0/2)}, \tag{41}$$

where $\mathcal{N}$ is a normalization factor. The parameter $\bar{M}$ is a nuisance parameter and should be marginalized (integrated out) leading to a new $\bar{\chi}^2$ defined as

$$\bar{\chi}^2 = -2\ln \int_{-\infty}^{+\infty} e^{-\chi^2/2d\bar{M}}. \tag{42}$$

Using Eqs. (40) and (42), we find

$$\bar{\chi}^2(X_0) = \chi^2(\bar{M} = 0, X_0) - \frac{B(X_0)^2}{C} + \ln(C/2\pi), \tag{43}$$

where

$$B(X_0) = \sum_i \frac{[\mu_{\mathrm{obs}}(z_i) - \mu_{\mathrm{th}}(z_i; X_0, \bar{M} = 0)]}{\sigma_i^2}, \tag{44}$$

and

$$C = \sum_i \frac{1}{\sigma_i^2}. \tag{45}$$

Equivalent to marginalization is the minimization of $\bar{\chi}^2$ with respect to $\bar{M}$. One can show that $\bar{\chi}^2$ can be expanded in terms of $\bar{M}$:

$$\chi^2_{\mathrm{SNIa}}(X_0) = \chi^2(\bar{M} = 0, X_0) - 2\bar{M}B + \bar{M}^2 C, \tag{46}$$

which has a minimum value for $\bar{M} = B/C$ and results in

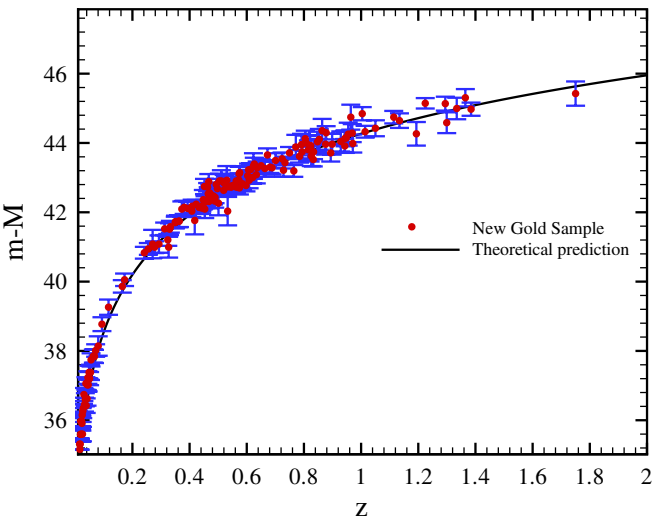

FIG. 7 (color online). The best fit of distance modulus as a function of redshift to the Supernova Type Ia new gold sample.

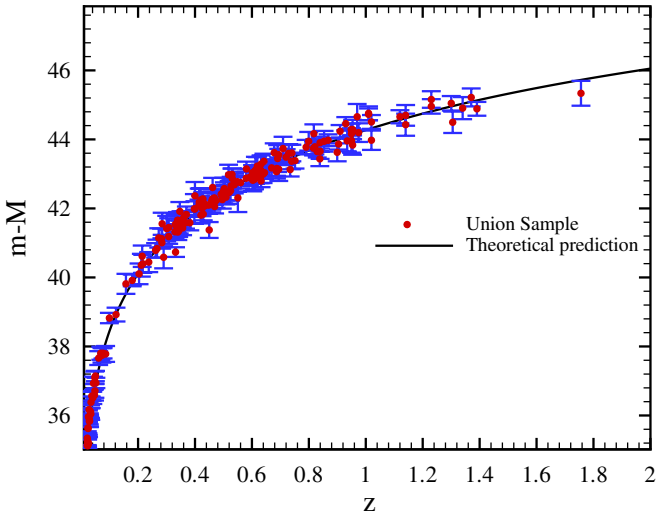

FIG. 8 (color online). The best fit of distance modulus as a function of redshift to the Supernova Type Ia union sample.

$$\mathcal{X}^2_{\mathrm{SNIa}}(X_0) = \mathcal{X}^2(\bar{M} = 0, X_0) - \frac{B(X_0)^2}{C}. \qquad (47)$$

Using Eq. (47) we can find the best fit values of model parameters, minimizing $\mathcal{X}^2_{\mathrm{SNIa}}(X_0)$, with the priors given in Table I. Figures 7 and 8 represent the best fit to the Supernova Type Ia new gold sample and union sample, respectively. The best fit values for the free parameter of the model for two cases are $n = 2.01^{+0.72}_{-0.67}$, $X_0 = 6.45^{+1.13}_{-1.51}$, and $\Omega_m = 0.67^{+0.64}_{-0.64}$ for the new gold sample and $n = 1.63^{+0.76}_{-0.92}$, $X_0 = 6.09^{+1.32}_{-2.86}$, and $\Omega_m = 0.47^{+0.69}_{-0.47}$ for mixed Gold-SNLS data. Figures 9 and 10 represent the likelihood functions in terms of n and X_0.

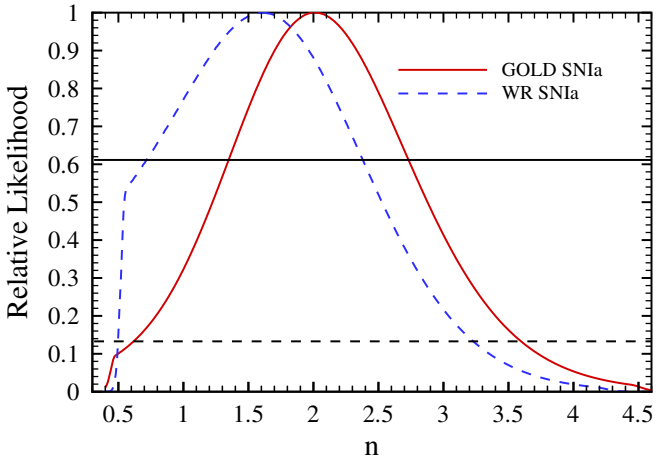

FIG. 9 (color online). Marginalized likelihood functions of $f(R)$ modified gravity model free parameter, n. The solid and dash lines correspond to the likelihood function of fitting the model with SNIa data new gold sample and union data set, respectively. The intersections of the curves with the horizontal solid and dashed lines give the bounds with 1σ and 2σ level of confidence, respectively.

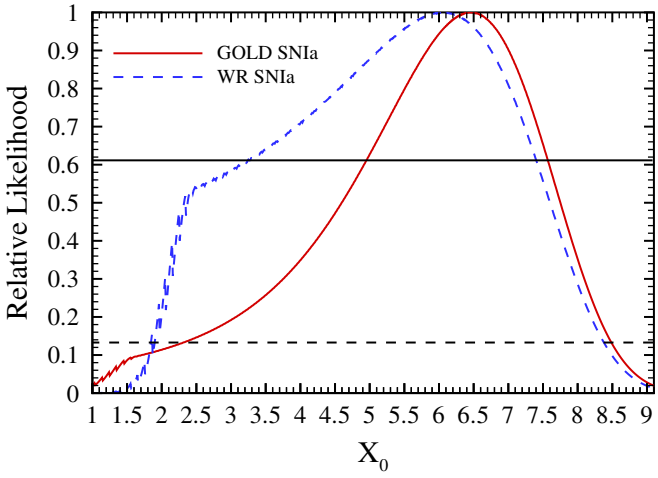

FIG. 10 (color online). Marginalized likelihood functions of $f(R)$ modified gravity model free parameter, X_0. The solid and dash lines correspond to the likelihood function of fitting the model with SNIa data new gold sample and union data set, respectively. The intersections of the curves with the horizontal solid and dashed lines give the bounds with 1σ and 2σ level of confidence, respectively.

B. CMBR shift parameter

Another dynamical parameter that is used in recent cosmological tests is the CMB shift parameter. Before the last scattering epoch, the baryons and photons were tightly coupled through the electromagnetic interaction. This coupled fluid was under the influence of two major forces of (a) the gravitational pull of matter, and (b) the outleading pressure of photons. The fingerprint of this competition leads to the familiar spectrum of peaks and troughs on the CMB map. Here the main peak is the so-called acoustic peak. The odd peaks of the CMB anisotropy spectrum correspond to the maximum compression of the fluid, the even ones to the rarefaction [10].

In an idealized model of the fluid, there is an analytic relation for the location of the mth peak: $l_m \approx m l_A$ [11,12], where l_A is the acoustic scale which may be calculated analytically and depends on both pre- and post-recombination physics as well as the geometry of the universe. The acoustic scale corresponds to the Jeans length of photon-baryon structures at the last scattering surface some ~379 Kyr after the big bang [13]. The apparent angular size of the acoustic peak can be obtained by dividing the comoving size of the sound horizon at the decoupling epoch $r_s(z_{\mathrm{dec}})$ by the comoving distance of observer to the last scattering surface $r(z_{\mathrm{dec}})$:

$$\theta_A = \frac{\pi}{l_A} \equiv \frac{r_s(z_{\mathrm{dec}})}{r(z_{\mathrm{dec}})}. \qquad (48)$$

The numerator of Eq. (48) corresponds to the distance that the perturbation of pressure can travel from the big bang to up to the last scattering surface, which is defined as the integral below:

$$r_s(z_{\rm dec}) = \int_{z_{\rm dec}}^{\infty} \frac{v_s(z')dz'}{H(z')/H_0} \tag{49}$$

where $v_s(z)^{-2} = 3 + 9/4 \times \rho_b(z)/\rho_{\rm rad}(z)$ is the sound velocity in the unit of speed of light from the big bang up to the last scattering surface [11,14], $z_{\rm dec}$ is the redshift of the last scattering surface.

Changing the parameters of the model can change the size of the apparent acoustic peak and subsequently the position of $l_A \equiv \pi/\theta_A$ in the power spectrum of temperature fluctuations on CMB. The simple relation $l_m \approx m l_A$, however, does not hold very well for the first peak, although it is better for higher peaks [2]. Driving effects from the decay of the gravitational potential as well as contributions from the Doppler shift of the oscillating fluid introduce a shift in the spectrum. A good parametrizations for the location of the peaks and troughs is given by

$$l_m = l_A(m - \phi_m) \tag{50}$$

where ϕ_m is a phase shift determined predominantly by prerecombination physics, and is independent of the geometry of the Universe. Instead of the peak locations of the power spectrum of CMB, one can use another model-independent parameter, which is the so-called shift parameter $\mathcal{R}$, as

$$\mathcal{R} = \frac{\omega_m^{1/2}}{\omega_k^{1/2}} \sin n_k(\omega_k r) \tag{51}$$

where $\sin n_k(x) = \sin(x)$, x, $\sinh(x)$ for $k = -1, 0, 1$. For the case of a flat universe, which is our concern, the shift parameter reduces to the simpler formula of

$$\mathcal{R} = \sqrt{\Omega_m H_0^2} \int_0^{z_{\rm dec}} \frac{dz}{H(z)}. \tag{52}$$

Now we change the variable from the redshift to X and rewrite the above expression in terms of dimensionless parameter X and take the integral from the value of X at the present time as the lower limit of the integral and the value of X at the decoupling time as the upper limit:

$$\mathcal{R} = \frac{\Omega_m^{1/6}}{3^{4/3}} \int_{X_p}^{X_{\rm dec}} \frac{F' - XF''}{(2F - XF')^{2/3}} \frac{dX}{\mathcal{H}(X)}. \tag{53}$$

The observed result of the CMB experiment is $\mathcal{R} = 1.716 \pm 0.062$ [13]. It is worthwhile to mention that the dimensionless parameter $\mathcal{R}$ is independent of the Hubble constant. We compare the observed shift parameter with that of the model using the likelihood analyzing, minimizing χ^2 defined as

$$\chi^2_{\rm CMB} = \frac{[\mathcal{R}_{\rm obs} - \mathcal{R}_{\rm the}]^2}{\sigma^2_{\rm CMB}}. \tag{54}$$

C. Baryon acoustic oscillations

Another geometrical cosmological probe which determines the distance-redshift relation is BAO. The physics governing the production of BAO is well understood. Acoustic peaks occurred because cosmological perturbations excite sound waves in initial relativistic plasma in the early epoch of the Universe. Dark matter perturbations grow in place while the baryonic matter perturbations were carried out in an expanding spherical wave because of their interaction with photons. At the recombination epoch, when the photons started to decouple from the baryonic matter, the shell of the baryonic matter perturbation sphere was nearly 150 Mpc in the comoving frame. From the linear structure formation theories, this scale should not be changed until the present time. The structure formation theory predicts that this 150 Mpc imprint of baryonic matter remains in the correlation function of the density contrast and can be seen in the large-scale surveys.

By knowing the size of acoustic oscillation, one can measure the angular distance to this structure. The large-scale correlation function measured from 46 748 luminous red galaxies spectroscopic sample of SDSS include a clear peak at 100 $\rm Mpch^{-1}$ [15]. The corresponding comoving scale of the sound horizon shell is about 150 Mpc in radius. A dimensionless and H_0 independent parameter for constraining the cosmological models has been proposed in literatures [15] as follows:

$$\mathcal{A} = \sqrt{\Omega_m}\left[\frac{H_0 D_L^2(z_{\rm sdss}; X_0)}{H(z_{\rm sdss}; X_0) z_{\rm sdss}^2 (1 + z_{\rm sdss})^2}\right]^{1/3}. \tag{55}$$

or in simpler form

$$\mathcal{A} = \sqrt{\Omega_m}\mathcal{H}(X)^{-(1/3)}\left[\frac{1}{z_{\rm sdss}} \int_0^{z_{\rm sdss}} \frac{dz}{\mathcal{H}(X)}\right]^{2/3}. \tag{56}$$

We rewrite the above dimensionless quantity in terms of modified gravity model parameters as

$$\mathcal{A} = \sqrt{\Omega_m}\mathcal{H}(X)^{-(1/3)} \times \left[\frac{(3\Omega_m)^{-(1/3)}}{3 z_{\rm sdss}} \int_{X_p}^{X_{\rm sdss}} \frac{(F' - XF'')dX}{\mathcal{H}(X)(2F - XF')^{2/3}}\right]^{2/3} \tag{57}$$

Now we can put a constraint on the $f(R)$ modified gravity model using the value of $\mathcal{A} = 0.469 \pm 0.017$ from luminous red galaxies observation at $z_{\rm SDSS} = 0.35$ [15]. It is worthwhile to mention that the procedure above presented in literature is well proposed for dark energy models in which the Ω_m has the same definition in standard cosmology. In contrast to the dark energy models in gravity theories in the Palatini formalism, Ω_m is a conventional dimensionless parameter and does not have the same role as in dark Energy models, considering the well-known fact that $\Omega_m = 1$ does not correspond to a flat universe as in standard FRW equations. Consequently, in order to not include the weak model dependence of the dimensionless parameter $\mathcal{A}$, we will use another similar approach, pro-

posed by Percival *et al.* [16]. This method constrains general cosmological models by using BAO distance measurement from galaxy samples covering different redshift ranges. Measuring the distance redshift relation at two redshifts of $z = 0.2$ and $z = 0.35$ for clustering of SDSS luminous red galaxies enables us to define a new dimensionless parameter as

$$\mathcal{B} = \frac{D_V(z = 0.35)}{D_V(z = 0.20)} \tag{58}$$

where D_V is given by

$$D_V = \left[\frac{(1 + z)^2 d_A^2 cz}{H(z)}\right]^{1/3}, \tag{59}$$

and d_A is the angular diameter distance. The observational values for two different redshifts are reported in [16] with 1σ error:

$$\frac{r_s}{D_V(z = 0.20)} = 0.1980 \pm 0.0058 \tag{60}$$

$$\frac{r_s}{D_V(z = 0.35)} = 0.1094 \pm 0.0033 \tag{61}$$

where r_s is the comoving sound horizon scale at the recombination epoch. Considering that BAO measurements have the same measured scale at all redshifts, then we have a numerical value for $\mathcal{B}$ as

$$\mathcal{B} = \frac{D_V(z = 0.35)}{D_V(z = 0.2)} = 1.812 \pm 0.060. \tag{62}$$

Now we convert the comoving angular diameter distance to luminosity distance D_L and calculate D_L in terms of the dimensionless Hubble parameter in modified gravity

$$\mathcal{B} = \left[\frac{\mathcal{H}(z = 0.20) D_L{}^2(z = 0.35) 0.35(1 + 0.2)^2}{\mathcal{H}(z = 0.35) D_L{}^2(z = 0.20) 0.2(1 + 0.35)^2}\right]^{1/3}. \tag{63}$$

We use χ^2 as one more fitting parameter with the observed value of $\mathcal{B} = 1.812 \pm 0.060$. This observation permits us to add one more term to χ^2 from that of SNIa and CMB-shift parameter by minimizing

$$\chi^2_{\rm BAO} = \frac{(\mathcal{B}_{\rm obs} - \mathcal{B}_{\rm th})^2}{\sigma^2_{\rm BAO}}. \tag{64}$$

This is the third geometrical parameter we will use to constrain the model.

D. Gas mass fraction of cluster of galaxies

Measurement of the ratio of X-ray emitting gas to the total mass in galaxy clusters ($f_{\rm gas}$) also is an indication of the acceleration of the Universe. This method can be used as another cosmological test to constraint the parameters of the model. Galaxy clusters are the largest objects in the Universe; the gas fraction in them is presumed to be constant and nearly equal to the baryon fraction in the Universe. Sasaki (1996) and Pen (1997) described how measurements of the apparent dependence of the baryonic mass fraction could also, in principle, be used to constrain the geometry and matter content of a universe [17,18]. The geometrical constraint arises from the dependence of the measured baryonic mass fraction value on the assumed angular diameter distance to the clusters [19]. The baryonic mass content of galaxy clusters is dominated by the X-ray emitting intercluster gas, the mass of which exceeds the mass of optically luminous material by a factor of 6 [20,21]. Let us define $f_{\rm gas}$ as

$$f_{\rm gas} = \frac{M_{\rm gas}}{M_{\rm tot}} \tag{65}$$

In the second step we want to replace the mass of gas by the baryonic mass considering that

$$M_b = (1 + \beta) M_{\rm gas}, \tag{66}$$

where from the observations we know $\beta = 0.19 h^{1/2}$ [20]. On the other hand, we assume that we are observing rich cluster of galaxies where the fraction of baryonic mass to the total mass has the same fraction as in the universe with a bias factor b. We substitute this assumption in Eq. (65) to achieve

$$f_{\rm gas} = \frac{b}{1 + \beta} \frac{\Omega_b}{\Omega_m}. \tag{67}$$

Using the distribution of gas and matter in cluster, Sasaki (1996) showed that the fraction of gas depends on angular distance with $f_{\rm gas} \propto D_A^{3/2}$ [17]. On the other hand, the fraction of gas obtained from the observation depends on the model we are assuming for the dynamics of the universe. It is assumed that $f_{\rm gas}$ should in reality be independent of the redshift. To determine the constraints on the proposed modified gravity action, we fit the $f_{\rm gas}$ data with a model that accounts for the expected apparent variation in $f_{\rm gas}(z)$ as the underlying cosmology is varied. We choose both SCDM (a flat universe with $\Omega_m = 1$ and $h = 0.5$) and ΛCDM as reference cosmology models. The ratio of gas fraction for a given model to the reference model is: $f_{\rm gas}^{(\rm ref)}/f_{\rm gas}^{(\rm mod)} = [D_A^{(\rm ref)}/D_A^{(\rm mod)}]^{3/2}$. On the other hand, using Eq. (67) for a given model, the gas fraction for a reference model is obtained by

$$f_{\rm gas}^{(\rm ref)} = \frac{b\Omega_b}{(1 + 0.19\sqrt{h})\Omega_m}\left[\frac{D_A^{\rm ref}(z)}{D_A^{\rm mod}(z)}\right]^{3/2}, \tag{68}$$

where superscripts (ref) correspond once to SCDM and then to the ΛCDM model [22]. We use χ^2 to compare gas fractions of observational and theoretical models as follows:

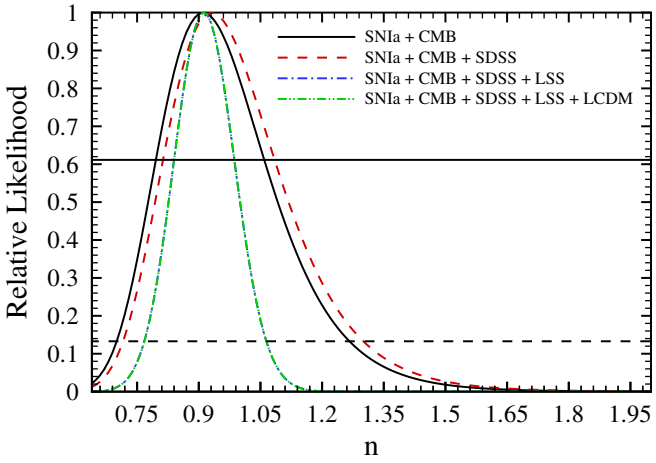

FIG. 11 (color online). Marginalized likelihood functions of $f(R)$ modified gravity model free parameter, n. The solid line corresponds to the joint analysis of SNIa data (new gold sample) and CMB, the dashed line shows the joint analysis of SNIa + CMB + SDSS data, the dash-dot line corresponds to SNIa + CMB + SDSS + LSS and the dash-dot-dot line indicates SNIa + CMB + SDSS + LSS + LCDM. The intersections of the curves with the horizontal solid and dashed lines give the bounds with 1σ and 2σ level of confidence, respectively. The results for two former analysis are very similar.

$$\chi_{\rm gas} = \frac{(f_{\rm gas}^{\rm obs} - f_{\rm gas}^{\rm the})^2}{\sigma_{\rm gas}^2}. \tag{69}$$

This is the fourth geometrical constraint.

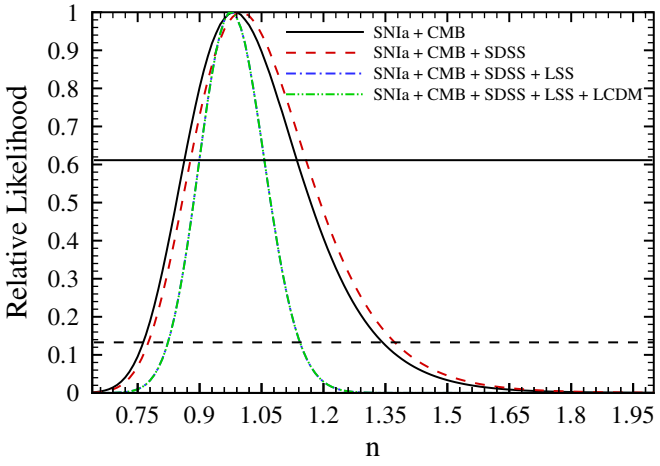

FIG. 12 (color online). Marginalized likelihood functions of $f(R)$ modified gravity model free parameter, n. The solid line corresponds to the joint analysis of SNIa data and CMB, the dashed line shows the joint analysis of SNIa + CMB + SDSS data, the dash-dot line corresponds to SNIa + CMB + SDSS + LSS and the dash-dot-dot line indicates SNIa + CMB + SDSS + LSS + LCDM. The intersections of the curves with the horizontal solid and dashed lines give the bounds with 1σ and 2σ level of confidence, respectively. The results for two former analyses are very similar.

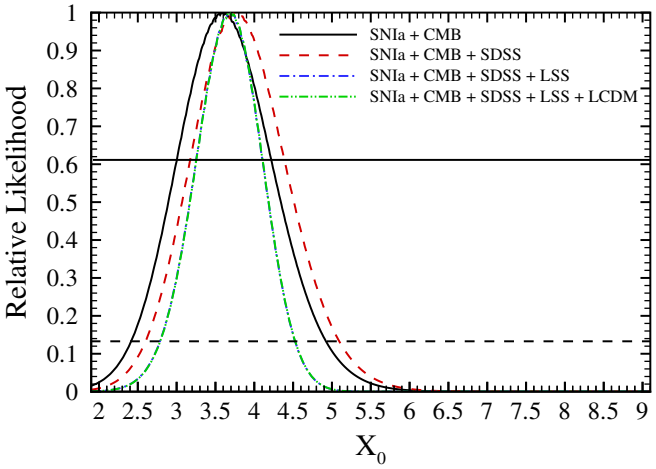

FIG. 13 (color online). Marginalized likelihood functions of $f(R)$ modified gravity model as a function of X_0. The solid line corresponds to the joint analysis of SNIa data (new gold sample) and CMB, the dashed line shows the joint analysis of SNIa + CMB + SDSS data, the dash-dot line corresponds to SNIa + CMB + SDSS + LSS and the dash-dot-dot line indicates SNIa + CMB + SDSS + LSS + LCDM. The intersections of the curves with the horizontal solid and dashed lines give the bounds with 1σ and 2σ level of confidence, respectively. The results for two former analyses are very similar.

E. Combined analysis: SNIa + CMB + BAO + GAS FRACTION

In this section we combine SNIa data (from SNIa new gold sample and mixed SNLS), CMB shift parameter from the WMAP, recently observed baryonic peak from the SDSS and 2dF, and the gas mass fraction in cluster of galaxies to constrain the parameter of the modified gravity model by minimizing the combined $\chi^2 = \chi^2_{\rm SNIa} + \chi^2_{\rm CMB} + \chi^2_{\rm BAO} + \chi^2_{\rm gas}$.

The best values of the parameters of the model from the fitting with data, including SNIa new sample are $n = 0.91^{+0.08}_{-0.07}$, $X_0 = 3.67^{+0.44}_{-0.42}$, and $\Omega_m = 0.29^{+0.10}_{-0.09}$ and data with including SNIa union sample results in $n = 0.98^{+0.08}_{-0.08}$, $X_0 = 4.39^{+0.38}_{-0.42}$, and $\Omega_m = 0.25^{+0.10}_{-0.010}$. Here we marginalized overall Hubble parameter in likelihood analysis. Figures 11 and 12 show the likelihood function as function of exponent n. Also Figs. 13 and 14 represent the likelihood function of X_0 in two different supernova data sets.

VI. CONSTRAINTS BY LARGE-SCALE STRUCTURES: DYNAMICAL PARAMETER

So far we have only considered the observational results related to the background evolution. In this section, using the linear approximation of structure formation, we obtain the growth index of structures and compare it with the result of observations by the 2-degree Field Galaxy Redshift Survey (2dFGRS). As we mentioned before, the

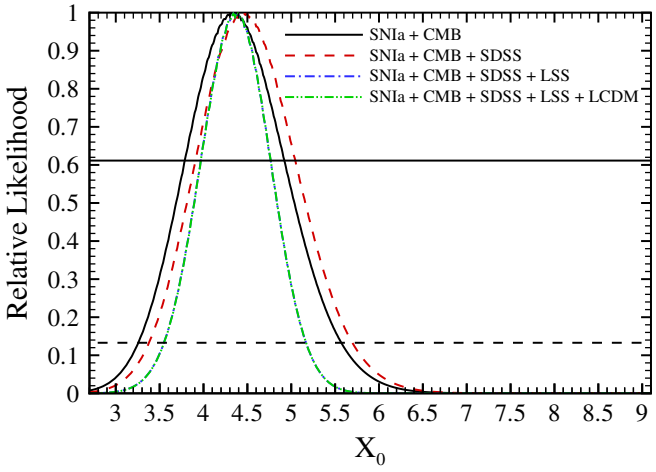

FIG. 14 (color online). Marginalized likelihood functions of the $f(R)$ modified gravity model as a function of X_0. The solid line corresponds to the analysis of SNIa data and CMB, the dashed line shows the joint analysis of SNIa + CMB + SDSS data, the dash-dot line corresponds to SNIa + CMB + SDSS + LSS and the dash-dot-dot line indicates SNIa + CMB + SDSS + LSS + LCDM. The intersections of the curves with the horizontal solid and dashed lines give the bounds with 1σ and 2σ level of confidence, respectively. The results for two former analyses are very similar.

evolution of the structures depends on both the dynamics of the background and the gravity law that governs the dynamics of particles inside the structure.

Here the evolution of structures in the modified gravity will be studied through the spherical collapse model. Recently a procedure has been put forward by Lue, Scoccimarro, and Starkman (2004) which relies on the assumption that Birkhoffs theorem holds in a more general setting of modified gravity theories. This procedure also is applied in the Palatini formalism of $f(R)$ gravity [23]. According to this procedure, it is assumed that the growth of large-scale structures can be modeled in terms of a uniform sphere of dust of constant mass. This structure evolves as a FRW universe. Using Birkhoffs theorem, the space-time at the empty exterior of this structure is then taken to be a Schwarzschild-like metric. The components of the exterior metric are then uniquely determined by smoothly matching the interior and exterior regions. In the Palatini formalism the metric outside the spherical distribution of matter depends on the density of matter which may modify the Newtonian limit of these theories; however, here we assume Schwarzschild-like Newtonian limit.

The continuity and Poisson equations for the density contrast $\delta = \delta\rho/\bar{\rho}$ in the cosmic fluid provide the evolution of density contrast in the linear approximation (i.e. $\delta \ll 1$) as

$$\ddot{\delta} + 2\frac{\dot{a}}{a}\dot{\delta} - 4\pi G\rho\delta = 0, \tag{70}$$

where the dot denotes the time derivative and we assume the size of structures to be larger than the Jeans length. The effect of a modified gravity results from the modification to the background dynamics, and we adopt the same Poisson equation for the weak field regime. In order to use the constraint from the large-scale structure, we rewrite the above equation in terms of X. So we have

$$\frac{d^2\delta}{da^2} + \frac{d\delta}{da}\left[\frac{3}{a} + \frac{\mathcal{H}'(X)}{\mathcal{H}(X)}\frac{dX}{da}\right] - \frac{3\Omega_m}{2\mathcal{H}^2(X)a^5}\delta = 0. \tag{71}$$

In the standard linear perturbation theory, the peculiar velocity field $\mathbf{v}$ is determined by the density contrast as

$$\mathbf{v}(\mathbf{x}) = H_0\frac{f}{4\pi}\int \delta(\mathbf{y})\frac{\mathbf{x}-\mathbf{y}}{|\mathbf{x}-\mathbf{y}|^3}d^3\mathbf{y}, \tag{72}$$

where the growth index f is defined by

$$f = \frac{d\ln\delta}{d\ln a}, \tag{73}$$

and it is proportional to the ratio of the second term of Eq. (70) (friction) to the third term (Poisson).

We use the evolution of the density contrast δ to compute the growth index of structure f, which is an important quantity for the interpretation of peculiar velocities of galaxies. Replacing the density contrast with the growth index in Eq. (72) results in the evolution of growth index as

$$\frac{df}{d\ln a} = \frac{3\Omega_m}{2a\mathcal{H}^2(X)} - f^2 - f\left[2 + \frac{a\mathcal{H}'(X)}{\mathcal{H}(X)}\frac{dX}{da}\right]. \tag{74}$$

To put constraint on the model using large structure data, we rely on the observation of 220 000 galaxies with the 2dFGRS experiment, which provides a numerical value for the growth index. By measurements of the two-point correlation function, the 2dFGRS team reported the redshift distortion parameter of $\beta = f/b = 0.49 \pm 0.09$ at $z = 0.15$, where b is the bias parameter describing the difference in the distribution of galaxies and their masses. Verde *et al.* (2003) used the bispectrum of 2dFGRS galaxies [24,25] and obtained $b_{\text{verde}} = 1.04 \pm 0.11$, which gave $f = 0.51 \pm 0.10$. Now we fit the growth index at $z = 0.15$ derived from the Eq. (74) with the observed value.

$$\chi^2_{\text{LSS}} = \frac{[f_{\text{obs}}(z = 0.15) - f_{\text{th}}(z = 0.15; X_0)]^2}{\sigma^2_{f_{\text{obs}}}}. \tag{75}$$

Finally, we do a likelihood analysis with considering all the observations and obtain the 2D distribution of a likelihood function in terms of n and X_0 in Fig. 17.

Perturbation theory

In the previous section we have seen the effect of modified gravity on the structure formation in the weak filed regime through the background effect. In this method, changing the dynamics of universe (i.e. scale factor) alters the formation of the large-scale structures.

In this section we study the relativist structure formation theory through the perturbation in the homogenous background metric and energy-momentum tensor. This approach may uncover whether modified gravity theories driving late-time acceleration predict any testable features on CMB or large-scale structures in linear or nonlinear regimes.

Let us consider a flat universe dominated by pressureless cold dark matter. We identify perturbation in conformally flat FRW space-time by ten elements as follows:

$$ds^2 = a^2(\eta)\{-(1+2\alpha)d\eta^2 - 2(\beta_{,i} + b_i)d\eta dx^i + [g^3_{ij} + 2(g^{(3)}_{ij}\phi + \gamma_{,ij} + c_{(i,j)}) + h_{ij}]dx^i dx^j\} \quad (76)$$

where η is the conformal time. α, β, γ, and ϕ are the scalar perturbations to the metric. b_i and c_i are divergenceless vectors where each one with 2 degrees of freedom and h_{ij} is a traceless–divergenceless symmetric 3×3 matrix with 2° of freedom.

On the other hand, perturbation of conservation of energy-momentum tensor results in the continuity and Euler equations as follows:

$$\dot{\delta} = -k\upsilon + a\kappa - 3H\alpha, \quad (77)$$

$$\dot{\upsilon} = -H\upsilon + k\alpha, \quad (78)$$

where $\kappa = 3a^{-1}(H\alpha - \dot{\phi}) - a^{-2}\Box\chi$ and $\chi = a(\beta + \dot{\gamma})$.

Using conformal gauge, the field equation for the density contrast in the modified gravity framework are obtained as [26]

$$\delta'' + \xi H\delta' - \zeta\left(\frac{H''}{H} - 2H'\right)\delta = 0 \quad (79)$$

where $'$ is the derivative with respect to the conformal time and $H = \frac{a'}{a} = \dot{a}$. ξ and ζ are defined as

$$\xi = 1 + \frac{2FF''H - 2F'^2H - 2FF'H'}{FH^2(2FH + F')}, \quad (80)$$

$$\zeta = 1 + \frac{H^2 - H'}{H'' - 2H'H}(1 - \xi) - \frac{F'H}{3(2FH + F')(H'' - 2H'H)}k^2, \quad (81)$$

where k is the wave number of structures in the universe. In the case of the Einstein-Hilbert action, $F' = F'' = 0$, which results in $\xi = 1$ and subsequently $\zeta = 1$. The differential equation governing the evolution of the density contrast in this case reduces to

$$\delta'' + H\delta' - \left(\frac{H''}{H} - 2H'\right)\delta = 0. \quad (82)$$

For comparison of Eqs. (79) and (82), we obtain the difference in the density contrast between the ΛCDM model and the modified gravity as indicated in Fig. 15

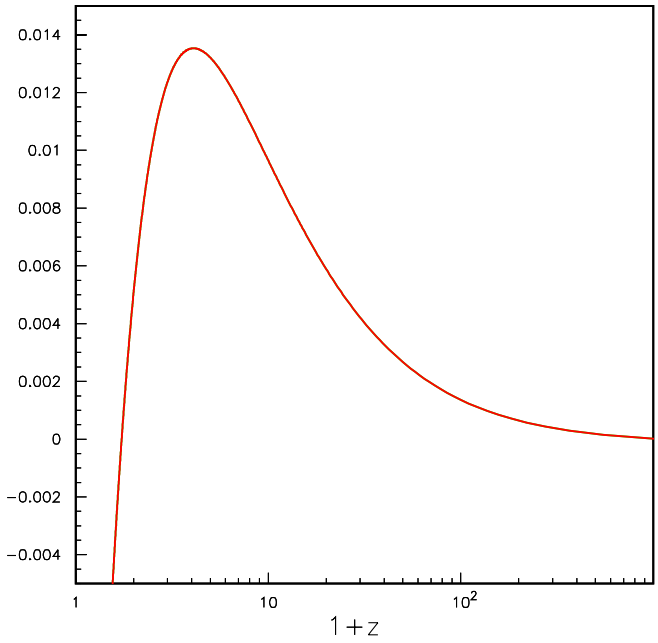

FIG. 15 (color online). Difference between the density contrast in the ΛCDM model and the modified gravity model. For larger redshifts the difference between these two solutions is negligible.

for a structure with the size of $k = 0.01$ Mpc^{-1}. For the larger scales, the third term in the Eq. (81) tends to zero and we get a smaller difference between the density contrast in these two solutions. In order to compare these results with data, more detailed simulation in the nonlinear regime of the structure formation is essential.

VII. AGE OF UNIVERSE

The age of the universe integrated from the big bang up to now for a flat universe in terms of free parameters of model n and X_0 is given by

$$t_0(X_p) = \int_0^{t_0} dt = \int_0^\infty \frac{dz}{(1+z)H(z)} = \frac{1}{3H_0}\int_{X_p}^\infty \frac{F' - XF''}{2F - XF'}\frac{dX}{\mathcal{H}(X)}. \quad (83)$$

Figure 16 shows the dependence of H_0t_0 (Hubble parameter times the age of universe) on X_0 for a flat universe. In the lower panel we show the same function for ΛCDM universe in terms of Ω_Λ for comparison. As we expected, X_0 in modified gravity behaves as a dark energy and increasing it makes a longer age for the universe, in the same direction as increasing the cosmological constant.

The "age crisis" is one the main reasons for the acceleration phase of the universe. The problem is that the universe's age in the CDM universe is less than the age of old stars in it. Studies on the old stars [27] suggest an age of 13^{+4}_{-2} Gyr for the universe. Richer *et al.* [28] and Hasen

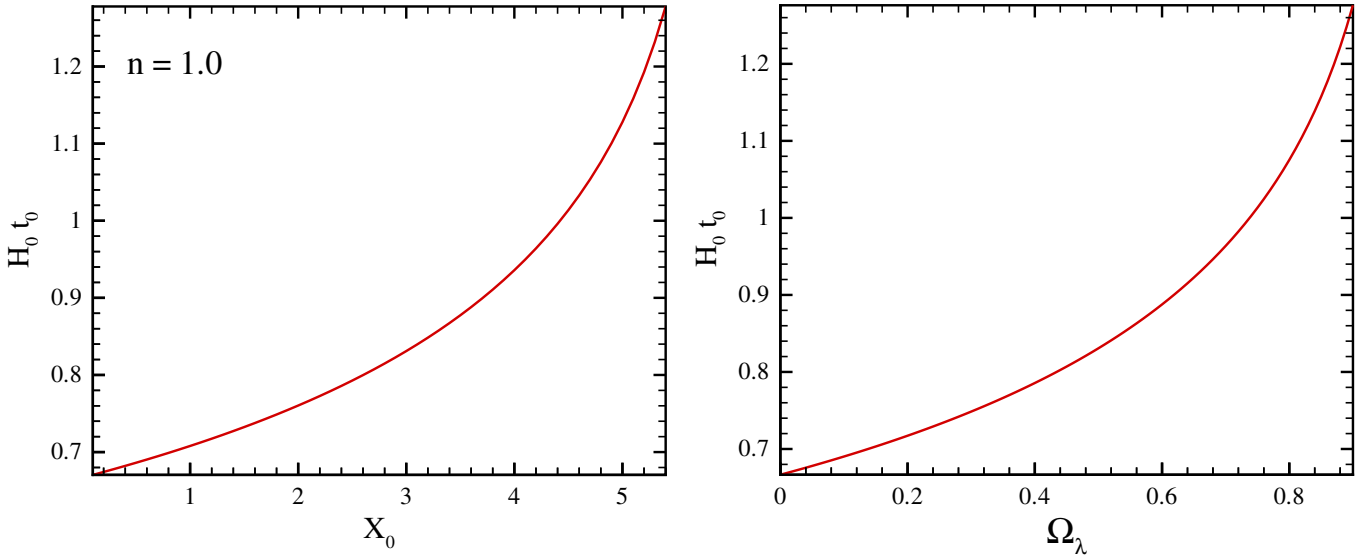

FIG. 16 (color online). H_0t_0 (age of universe times the Hubble constant at the present time) as a function of X_0 (upper panel). H_0t_0 for ΛCDM versus Ω_λ (lower panel). Increasing X_0 gives a longer age for the universe. This behavior is the in the same direction as in the ΛCDM universe.

et al. [29] also proposed an age of 12.7 ± 0.7 Gyr, using the white dwarf cooling sequence method.

We use the age of universe in this model for the consistency test and compare the age of universe with the age of old stars and old high redshift galaxies (OHRG) in various redshifts. Table II shows that the age of universe from the combined analysis of SNIa + CMB + SDSS + LSS is $14.69^{+0.29}_{-0.28}$ Gyr and $13.45^{+0.30}_{-0.28}$ Gyr for the new gold sample and union data sample, respectively. These values are in agreement with the age of old stars [27]. Here we take three OHRG for comparison with the modified gravity model considering the best fit parameters, namely, the LBDS 53W091, a 3.5-Gyr old radio galaxy at $z = 1.55$ [30], the LBDS 53W069 a 4.0-Gyr old radio galaxy at $z = 1.43$ [31], and a quasar, APM 08279 + 5255 at $z = 3.91$ with an age of $t = 2.1^{+0.9}_{-0.1}$ Gyr [32]. To quantify the age-consistency test we introduce the expression τ as

$$\tau = \frac{t(z; X_0)}{t_{\rm obs}} = \frac{t(z; X_0)H_0}{t_{\rm obs}H_0}, \tag{84}$$

where $t(z)$ is the age of universe, obtained from the Eq. (83) and $t_{\rm obs}$ is an estimation for the age of an old cosmological object. In order to have a compatible age for the universe we should have $\tau > 1$. Table III reports the value of τ for three mentioned OHRGs with various observations. We see that $f(R)$ modified gravity with the parameters from the combined observations provides a compatible age for the

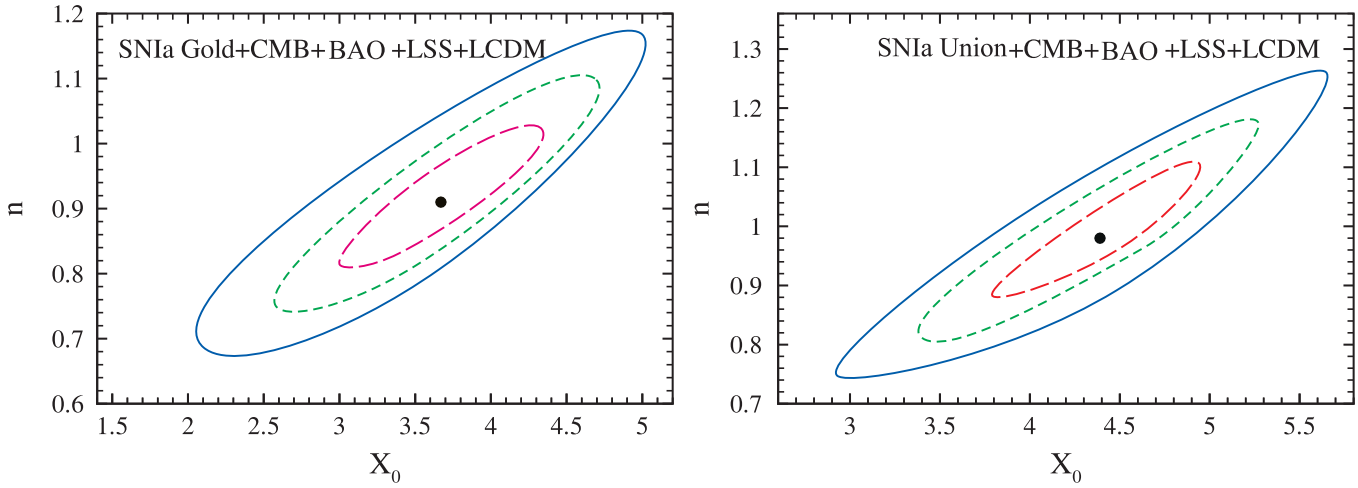

FIG. 17 (color online). Joint likelihood function in terms of n and X_0 considering all the observable data. In the upper panel the SNIa data is taken from the gold sample and in the lower panel the data is the union sample.

TABLE II. The best values for the parameters of modified gravity with the corresponding age for the universe from fitting with SNIa from new Gold sample and Union data sample, SNIa + CMB, SNIa + CMB + BAO, SNIa + CMB + BAO + LSS and SNIa + CMB + BAO + LSS + GAS(ΛCDM) experiments at one and two σ confidence level. The value of Ω_m is determined according to Eq. (25).

Observation	n	X_0	Ω_m	Age (Gyr)
SNIa(new Gold)	$2.01^{+0.72}_{-0.67}$	$6.45^{+1.13}_{-1.51}$	$0.67^{+0.64}_{-0.65}$	$12.99^{+4.42}_{-6.24}$
	$2.01^{+1.06}_{-0.95}$	$6.45^{+1.53}_{-2.36}$	$0.67^{+0.90}_{-1.01}$	$12.99^{+7.17}_{-7.17}$
SNIa(new Gold) + CMB	$0.91^{+0.15}_{-0.11}$	$3.58^{+0.64}_{-0.58}$	$0.31^{+0.19}_{-0.14}$	$14.55^{+2.02}_{-1.68}$
	$0.91^{+0.23}_{-0.16}$	$3.58^{+0.92}_{-0.72}$	$0.31^{+0.28}_{-0.20}$	$14.55^{+3.40}_{-2.53}$
SNIa(new Gold) + CMB + BAO	$0.93^{+0.16}_{-0.12}$	$3.76^{+0.63}_{-0.59}$	$0.30^{+0.19}_{-0.15}$	$14.72^{+2.14}_{-1.89}$
	$0.93^{+0.24}_{-0.22}$	$3.76^{+0.91}_{-0.83}$	$0.30^{+0.29}_{-0.25}$	$14.72^{+3.29}_{-1.43}$
SNIa(new Gold) + CMB + SDSS + LSS	$0.91^{+0.08}_{-0.07}$	$3.67^{+0.44}_{-0.42}$	$0.29^{+0.10}_{-0.09}$	$14.73^{+1.31}_{-1.51}$
	$0.91^{+0.11}_{-0.10}$	$3.67^{+0.61}_{-0.61}$	$0.29^{+0.15}_{-0.14}$	$14.73^{+1.87}_{-1.68}$
SNIa(new Gold) + CMB + SDSS + LSS + GAS(ΛCDM)	$0.91^{+0.08}_{-0.07}$	$3.67^{+0.44}_{-0.42}$	$0.29^{+0.10}_{-0.09}$	$14.73^{+1.31}_{-1.51}$
	$0.91^{+0.11}_{-0.10}$	$3.67^{+0.61}_{-0.61}$	$0.29^{+0.15}_{-0.14}$	$14.73^{+1.87}_{-1.68}$
SNIa (UNION)	$1.63^{+0.76}_{-0.92}$	$6.09^{+1.32}_{-2.86}$	$0.47^{+0.69}_{-0.47}$	$14.27^{+7.31}_{-7.31}$
	$1.63^{+1.09}_{-1.10}$	$6.09^{+1.75}_{-3.95}$	$0.47^{+0.90}_{-0.47}$	$14.27^{+8.34}_{-8.34}$
SNIa(UNION) + CMB	$0.99^{+0.15}_{-0.13}$	$4.36^{+0.57}_{-0.58}$	$0.26^{+0.17}_{-0.15}$	$15.47^{+2.40}_{-2.43}$
	$0.99^{+0.22}_{-0.17}$	$4.36^{+0.83}_{-0.80}$	$0.26^{+0.25}_{-0.20}$	$15.47^{+3.77}_{-3.50}$
SNIa(UNION) + CMB + BAO	$1.00^{+0.16}_{-0.12}$	$4.45^{+0.60}_{-0.54}$	$0.26^{+0.18}_{-0.14}$	$15.59^{+2.64}_{-2.28}$
	$1.00^{+0.24}_{-0.17}$	$4.45^{+0.86}_{-0.77}$	$0.26^{+0.27}_{-0.20}$	$15.59^{+4.17}_{-3.59}$
SNIa(UNION) + CMB + BAO + LSS	$0.98^{+0.08}_{-0.08}$	$4.39^{+0.38}_{-0.42}$	$0.25^{+0.10}_{-0.10}$	$15.67^{+1.52}_{-1.57}$
	$0.98^{+0.11}_{-0.11}$	$4.39^{+0.55}_{-0.60}$	$0.25^{+0.14}_{-0.14}$	$15.67^{+2.27}_{-2.25}$
SNIa(UNION) + CMB + BAO + LSS GAS(ΛCDM)	$0.98^{+0.08}_{-0.08}$	$4.39^{+0.38}_{-0.42}$	$0.25^{+0.10}_{-0.10}$	$15.67^{+1.52}_{-1.57}$
	$0.98^{+0.11}_{-0.11}$	$4.39^{+0.55}_{-0.60}$	$0.25^{+0.14}_{-0.14}$	$15.67^{+2.27}_{-2.25}$

TABLE III. The value of τ for three high redshift objects, using the parameters of the model derived from fitting with the observations at one and two σ level of confidences.

Observation	LBDS 53W069 $z = 1.43$	LBDS 53W091 $z = 1.55$	APM 08279 + 5255 $z = 3.91$
SNIa (new Gold)	$0.81^{+0.48}_{-0.81}$	$0.90^{+0.52}_{-0.90}$	$0.53^{+0.36}_{-0.53}$
	$0.81^{+0.81}_{-0.81}$	$0.90^{+0.90}_{-0.90}$	$0.53^{+0.53}_{-0.53}$
SNIa(new Gold) + CMB	$1.18^{+0.29}_{-0.25}$	$1.26^{+0.31}_{-0.28}$	$0.81^{+0.23}_{-0.41}$
	$1.18^{+0.45}_{-0.39}$	$1.26^{+0.49}_{-0.43}$	$0.81^{+0.34}_{-0.49}$
SNIa(new Gold) + CMB + BAO	$1.20^{+0.31}_{-0.29}$	$1.28^{+0.34}_{-0.31}$	$0.82^{+0.42}_{-0.24}$
	$1.20^{+0.48}_{-0.46}$	$1.28^{+0.52}_{-0.48}$	$0.82^{+0.50}_{-0.28}$
SNIa(new Gold) + CMB + BAO + LSS	$1.21^{+0.19}_{-0.17}$	$1.29^{+0.20}_{-0.18}$	$0.83^{+0.38}_{-0.14}$
	$1.21^{+0.27}_{-0.25}$	$1.29^{+0.29}_{-0.27}$	$0.83^{+0.43}_{-0.41}$
SNIa(new Gold) + CMB + BAO + LSS + GAS	$1.21^{+0.19}_{-0.17}$	$1.29^{+0.20}_{-0.18}$	$0.83^{+0.38}_{-0.14}$
	$1.21^{+0.27}_{-0.25}$	$1.29^{+0.29}_{-0.27}$	$0.83^{+0.43}_{-0.41}$
SNIa (UNION)	$0.97^{+1.06}_{-0.97}$	$1.02^{+1.13}_{-1.02}$	$0.63^{+0.73}_{-0.63}$
	$0.97^{+1.15}_{-0.97}$	$1.02^{+1.49}_{-1.02}$	$0.63^{+0.83}_{-0.63}$
SNIa(UNION) + CMB	$1.23^{+0.34}_{-0.36}$	$1.31^{+0.37}_{-0.40}$	$0.84^{+0.44}_{-0.30}$
	$1.23^{+0.55}_{-0.54}$	$1.31^{+0.60}_{-0.58}$	$0.84^{+0.55}_{-0.45}$
SNIa(UNION) + CMB + BAO	$1.24^{+0.38}_{-0.34}$	$1.33^{+0.41}_{-0.37}$	$0.84^{+0.46}_{-0.28}$
	$1.24^{+0.62}_{-0.55}$	$1.33^{+0.67}_{-0.60}$	$0.84^{+0.60}_{-0.47}$
SNIa(UNION) + CMB + BAO + LSS	$1.26^{+0.22}_{-0.23}$	$1.34^{+0.24}_{-0.25}$	$0.86^{+0.40}_{-0.19}$
	$1.26^{+0.33}_{-0.33}$	$1.34^{+0.36}_{-0.36}$	$0.86^{+0.44}_{-0.27}$
SNIa(UNION) + CMB + BAO + LSS + GAS	$1.26^{+0.22}_{-0.23}$	$1.34^{+0.24}_{-0.25}$	$0.86^{+0.40}_{-0.19}$
	$1.26^{+0.33}_{-0.33}$	$1.34^{+0.36}_{-0.36}$	$0.86^{+0.44}_{-0.27}$

universe, compared to the age of old objects, while the SNLS data result in a shorter age for the universe. Once again, APM 08279 + 5255 at $z = 3.91$ has a longer age than the universe but gives better results than some of the modified gravity models [33].

VIII. CONCLUSION

In this work we proposed the action of $f(R) = (R^n - R_0^n)^{1/n}$ to obtain the dynamics of the universe. We used the Palatini formalism to extract the field equation. The advantage of this formalism is that the field equation is a second-order differential equation and in the solar system scales we can recover a Schwarzschild–de Sitter space with an effective cosmological constant compatible with the observations. The other advantage of the Palatini formalism is that it does not suffer from the curvature instability as pointed out in [34].

We used cosmological tests based on background dynamics such as Supernova Type Ia, CMB-shift parameter, baryonic acoustic oscillation, and gas mass fraction of the cluster of galaxies. We also used data from the structure formation to put constraints on the parameters of the model. Table II represents constraints on the parameters of model considering the observational data and their combination. We also showed that this model provides an age for the universe sufficiently longer than the age of old astrophysical objects.

Comparing this model with the observations we put the constraint of $n = 0.98^{+0.08}_{-0.08}$ for the exponent of action and $X_0 = 4.39^{+0.38}_{-0.38}$ or equivalently $\Omega_m = 0.25^{+0.10}_{-0.10}$. The best value for this model shows that a standard ΛCDM model also resides in this range of solutions. Our result is in agreement with the recent work by Kowalski *et al.* (2008) where they also obtained almost a ΛCDM universe with a nearly constant equation of state for a dark energy model [35].

[1] T. M. Davis *et al.*, Astrophys. J. **666**, 716 (2007); E. L. Wright, Astrophys. J. **664**, 633 (2007); M. Sahlen, A. R. Liddle, and D. Parkinson, Phys. Rev. D **75**, 023502 (2007).

[2] S. M. Carroll, V. Duvvuri, M. Trodden, and M. S. Turner, Phys. Rev. D **70**, 043528 (2004); S. Nojiri and S. D. Odintsov, Gen. Relativ. Gravit. **36**, 1765 (2004); M. E. Soussa and R. P. Woodard, Gen. Relativ. Gravit. **36**, 855 (2004); G. Allemandi, A. Borowiec, and M. Francaviglia, Phys. Rev. D **70**, 103503 (2004); D. A. Easson, Int. J. Mod. Phys. A **19**, 5343 (2004); S. M. Carroll, A. De Felice, V. Duvvuri, D. A. Easson, M. Trodden, and M. S. Turner, Phys. Rev. D **71**, 063513 (2005); S. Carloni, P. K. S. Dunsby, S. Capozziello, and A. Troisi, Classical Quantum Gravity **22**, 4839 (2005); S. Capozziello, V. F. Cardone, and A. Troisi, Phys. Rev. D **71**, 043503 (2005); G. Cognola, E. Elizalde, S. Nojiri, S. D. Odintsov, and S. Zerbini, J. Cosmol. Astropart. Phys. 02 (2005) 010; S. Nojiri, S. D. Odintsov, and S. Tsujikawa, Phys. Rev. D **71**, 063004 (2005); T. Clifton and J. D. Barrow, Phys. Rev. D **72**, 103005 (2005); S. Das, N. Banerjee, and N. Dadhich, Classical Quantum Gravity **23**, 4159 (2006); S. Capozziello, V. F. Cardone, E. Elizalde, S. Nojiri, and S. D. Odintsov, Phys. Rev. D **73**, 043512 (2006); T. P. Sotiriou, Classical Quantum Gravity **23**, 5117 (2006); A. De Felice, M. Hindmarsh, and M. Trodden, J. Cosmol. Astropart. Phys. 08 (2006) 005; S. Nojiri and S. D. Odintsov, Phys. Rev. D **74**, 086005 (2006); A. F. Zakharov, A. A. Nucita, F. De Paolis, and G. Ingrosso, Phys. Rev. D **74**, 107101 (2006); P. Zhang, Phys. Rev. D **73**, 123504 (2006); K. Atazadeh and H. R. Sepangi, Int. J. Mod. Phys. D **16**, 687 (2007); S. M. Carroll, I. Sawicki, A. Silvestri, and M. Trodden, New J. Phys. **8**, 323 (2006); D. Huterer and E. V. Linder, Phys. Rev. D **75**, 023519 (2007); V. Faraoni, Phys. Rev. D **74**, 104017 (2006); Y. S. Song, W. Hu, and I. Sawicki, Phys. Rev. D **75**, 044004 (2007); R. Bean, D. Bernat, L. Pogosian, A. Silvestri and M. Trodden, Phys. Rev. D **75**, 064020 (2007); T. Chiba, T. L. Smith, and A. L. Erickcek, Phys. Rev. D **75**, 124014 (2007); V. Faraoni and S. Nadeau, Phys. Rev. D **75**, 023501 (2007); S. Rahvar and Y. Sobouti, Mod. Phys. Lett. A **23**, 1929 (2008).

[3] T. Koivisto, Classical Quantum Gravity **23**, 4289 (2006).

[4] Sh. Baghram, M. Farhang, and S. Rahvar, Phys. Rev. D **75**, 044024 (2007).

[5] M. S. Movahed, Sh. Baghram, and S. Rahvar, Phys. Rev. D **76**, 044008 (2007).

[6] S. Perlmutter, M. S. Turner, and M. White, Phys. Rev. Lett. **83**, 670 (1999).

[7] B. P. Schmidt *et al.*, Astrophys. J. **507**, 46 (1998).

[8] A. G. Riess *et al.*, Astrophys. J. **607**, 665 (2004).

[9] A. G. Riess *et al.*, Astrophys. J. **659**, 98 (2007).

[10] W. Hu, N. Sugiyama, and J. Silk, Nature (London) **386**, 37 (1997).

[11] W. Hu and N. Sugiyama, Astrophys. J. **444**, 489 (1995).

[12] W. Hu, M. Fukugita, M. Zaldarriaga, and M. Tegmark, Astrophys. J. **549**, 669 (2001).

[13] D. N. Spergel, L. Verde, and H. V. Peiris, *et al.*, Astrophys. J. Suppl. **148**, 175 (2003).

[14] M. Doran, M. Lilley, J. Schwindt, and C. Wetterich, Astrophys. J. **559**, 501 (2001).

[15] D. J. Eisenstein *et al.*, Astrophys. J. **633**, 560 (2005).

[16] W. J. Percival *et al.*, Mon. Not. R. Astron. Soc. **381**, 1053 (2007).

[17] S. Sasaki, Publ. Astron. Soc. Jpn. **48**, L119 (1996).

[18] U. Pen, New Astron. Rev. **2**, 309 (1997).

[19] D. Rapetti, S. W. Allen, and A. Mantz, Mon. Not. R. Astron. Soc. **388**, 1265 (2008).
[20] S. D. M. White, J. F. Navarro, A. E. Evrard, and C. S. Frenk, Nature (London) **366**, 429 (1993).
[21] M. Fukugita, C. J. Hogan, and P. J. E. Peebles, Astrophys. J. **503**, 518 (1998).
[22] S. W. Allen *et al.*, Mon. Not. R. Astron. Soc. **353**, 457 (2004).
[23] K. Uddin, J. E Lidsey, and R. Tavakol, Classical Quantum Gravity **24**, 3951 (2007).
[24] L. Verde, M. Kamionkowski, J. J. Mohr, and A. J. Benson, Mon. Not. R. Astron. Soc. **321**, L7 (2001).
[25] O. Lahav, S. L. Bridle, and W. J. Percival (2dFGRS Team), Mon. Not. R. Astron. Soc. **333**, 961 (2002).
[26] Tomi Koivisto and Hannu Kurki-Suonio, Classical Quantum Gravity **23**, 2355 (2006).
[27] E. Carretta *et al.*, Astrophys. J. **533**, 215 (2000); B. Chaboyer and L. M. Krauss, Astrophys. J. Lett. **567**, L45 (2002).
[28] H. B. Richer *et al.*, Astrophys. J. **574**, L151 (2002).
[29] B. M. S. Hansen *et al.*, Astrophys. J. **574**, L155 (2002).
[30] J. Dunlop *et al.*, Nature (London) **381**, 581 (1996); H. Spinrad, Astrophys. J. **484**, 581 (1997).
[31] J. Dunlop, in *The Most Distant Radio Galaxies*, edited by H. J. A. Rottgering, P. Best, and M. D. Lehnert (Kluwer, Dordrecht, 1999), p. 71.
[32] G. Hasinger, N. Schartel, and S. Komossa, Astrophys. J. Lett. **573**, L77 (2002).
[33] M. S. Movahed and S. Rahvar, Phys. Rev. D **73**, 083518 (2006); S. Rahvar and M. S. Movahed, Phys. Rev. D **75**, 023512 (2007).
[34] T. P. Sotiriou, Phys. Lett. B **645**, 389 (2007).
[35] M. Kowalski *et al.*, Astrophys. J. **686**, 749 (2008).
[36] C. J. Copi, D. N. Schramm, and M. S. Turner, Science **267**, 192 (1995).
[37] W. L. Freedman *et al.*, Astrophys. J. Lett. **553**, 47 (2001).
[38] X. Zhang and F. Q. Wu, Phys. Rev. D **72**, 043524 (2005).